HHS Public Access

Author manuscript

Exp Neurol. Author manuscript; available in PMC 2016 August 01.

Published in final edited form as:

Exp Neurol. 2015 August ; 270: 88–94. doi:10.1016/j.expneurol.2014.10.008.

Fluoxetine is neuroprotective in slow-channel congenital myasthenic syndrome

Haipeng Zhu[1], **E. Grajales-Reyes**[2], **Vivianette Alicea Vázquez**[4], **KaReisha Robinson**[1], **Peter Pytel**[3], **Carlos A Báez-Pagán**[4], **Jose A Lasalde-Dominicci**[4], and **Christopher M Gomez**[*]

[1]Department of Neurology, The University of Chicago

[2]School of Medicine, Washington University, St Louis

[3]Department of Pathology, The University of Chicago

[4]Department of Biology, The University of Puerto Rico, Piedras Campus

Abstract

The slow-channel congenital myasthenic syndrome (SCS) is an inherited neurodegenerative disease caused mutations in the acetylcholine receptor (AChR) affecting neuromuscular transmission. Leaky AChRs lead to Ca^{2+} overload and degeneration of the neuromuscular junction (NMJ) attributed to activation of cysteine proteases and apoptotic changes of synaptic nuclei. Here we use transgenic mouse models expressing two different mutations found in SCS to demonstrate that inhibition of prolonged opening of mutant AChRs using fluoxetine not only improves motor performance and neuromuscular transmission but also prevents Ca^{2+} overload, activation of cysteine proteases, calpain, caspase-3 and 9 at endplates, and as a consequence, reduces subsynaptic DNA damage at endplates, suggesting a long term benefit to therapy. These studies suggest that prolonged treatment of SCS patients with open ion channel blockers that preferentially block mutant AChRs is neuroprotective.

Introduction

The slow-channel congenital myasthenic syndrome (SCS) is a degenerative neuromuscular disorder characterized by generalized fatigability, weakness, and wasting of face and limb muscles caused by point mutations in the muscle acetylcholine receptor (AChR). Mutant AChRs lead to disturbed gating, prolonged channel open times, postsynaptic Ca^{2+} overload, and degeneration of the neuromuscular junction (NMJ) (1–4). Previously, we showed that mutant AChRs are leaky and lead to Ca^{2+} overload of the postsynaptic region in conjunction with Ca^{2+} release from internal stores through the sarcoplasmic reticulum-resident type 1 inositol 1,4,5-triphosphate receptor (IP_3R_1) channel (5,6). Localized Ca^{2+} overload gives

[*]CORRESPONDING AUTHOR: Christopher M. Gomez, M.D., Ph.D., Department of Neurology, AMB S237, MC2030, University of Chicago, 5841, Chicago, Phone: 773-702-6390, Fax: 773-834-3232, gomez001@uchicago.edu.

rise to both functional and structural impairment of the NMJ and neuromuscular transmission (6–9). Therefore, prevention of prolonged opening of mutant AChR channel is a logical strategy in treatment of SCS.

Recently, both quinidine, and the anti-depressant, fluoxetine, have been shown to be of benefit in SCS by preferentially blocking mutant AChRs, apparently normalizing prolonged synaptic currents (10,11). Fluoxetine reduces prolonged opening of mutant AChR channels *in vitro* by several fold compared to wild-type and improves neuromuscular transmission in SCS (11–13). These reports demonstrate that inhibition of mutant AChR channel with fluoxetine functionally improves muscle strength and performance in SCS patients.

Detailed quantitative and structural outcome studies are difficult in humans. In this study, we used a well-established transgenic mouse model of SCS (mSCS) to assess the long-term benefits of fluoxetine therapy to functional and structural aspects of the NMJ. We showed that fluoxetine treatment remarkably attenuates the characteristic decrements of compound muscle action potentials associated with SCS and functionally improves quantitative measures of gait in mSCS. More importantly fluoxetine reduces Ca^{2+} overload at endplates, decreases activation of caspase-3 and -9 at the NMJ, and diminishes DNA damage in subsynaptic nuclei. These studies provide experimental evidence for the long-term, neuroprotective benefit of fluoxetine in SCS.

Material and Methods

Materials

Chemical reagents were purchased from Sigma Chemical Co. Cell culture materials were obtained from Gibco BRL Co. Laminin, Texas Red conjugated alphabungarotoxin (αBT) (TxR-αBT), and fluorescence-tagged secondary antibodies were purchased from Invitrogen Co. Secondary antibodies with horseradish peroxidase (HRP) were provided by GE Healthcare Bioscience Co. Primary antibodies were used to the following targets: phosphorylated H2AX (Ser139; 1:500; Millipore) and cleaved caspase-3 and -9 (1:200; Cell Signaling).

Animals and tissue preparation

4–6 month-old male wild type FVB mice and SCS transgenic mice (mSCS; εL269F and δS268F) were used in this study (15). Both were derived by targeted expression of the respective mutant cDNA to muscle using the muscle creatine kinase promoter (15). Both εL269F and δS268F mutations have been reported in patients with SCS (4,16). The clinical electrophysiological and pathological features of the transgenic mouse lines have been described in detail elsewhere (3,5,15,17). All drug treatments and surgical procedures followed the animal care and use protocols established by Institutional Animal Care and Use Committee (IACUC). Mice were anesthetized using ketamine and xylazine (18).

Drug administration

Fluoxetine hydrochloride (Sigma) in saline (0.9% w/v; Fisher Thermoscientific, Lake Forest, US) was administered intraperitoneally at the series of concentration of 2.4, 4.8, 7.2

and 9.6 μg/g daily to different mSCS groups for 9 days, respectively. Excised diaphragm of mSCS mice was treated *in vitro* with fluoxetine as 0.3, 0.9 and 1.5μM.

Tissue Staining and Imaging

Motor endplates in the serial sectioned TA muscle (tibialis anterior) were localized using a histochemical stain for cholinesterase (Koelle and Friedenwald, 1949) and Ca^{2+}-overloaded endplates were detected by glyoxal bis 2 hydroxyanil (GBHA) stain as described in (19,20). For immunohistochemistry, tissues sections were fixed in a 1:1 methanol-acetone mixture at −20°C for 30 min, air dried for 20 min, and incubated with blocking solution for 1hr at RT, followed by overnight incubation with primary antibody at 4°C. After washing, fluorescent secondary antibody in PBST (phosphate buffered saline and 0.05% Tween-20) for 1hr at RT. Confocal fluorescence microscopy was carried out under a TCS laser scanning microscope (Leica, Deerfield, IL). Optical sections of 0.5 μm were scanned for the *z*-axis. Image J was used to quantify the percentage of specific expression of antibody in NMJs of each sample.

Quantitative studies in tissue sections

Quantitation of the proportion of labeled NMJs in the TA muscle cryosections was carried out using sequential alternate sections stained for cholinesterase and test label (GBHA, pH2X and caspase 3 and 9) as described previously (3,15), using Image J (v5.3) for analysis.

Caspase activity assay

Caspase-3 and caspase-9 activities in muscle were measured using a firefly luciferase-based assay (Calpain-Glo™ Protease Assay; Caspase-Glo® 3/7 and 9 Assays; Promega). Muscle samples were homogenized as previously described (21) except for the addition of 10mM NH_4Cl and 10mM 3-methyladenine to the homogenization buffer to stabilize lysosomes and the proteasome complexes. Protein samples (20μg) were analyzed by luminometer (Turner BioSystems, Inc) in triplicate.

Electromyography (EMG)

Compound muscle action potentials (CMAPs) were detected and calculated as described previously using a Nicolet VikingQuest (Nicolet Biomedical, Inc) (7).

Electrophysiology

Two-electrode voltage clamp (TEVC) recordings of excised mouse diaphragm were performed as described (4,6,15). Briefly, after dissection diaphragm muscle was continuously perfused with a Tyrode's solution with a composition (in mM): 137 NaCl, 2.8 KCl, 1.8 $CaCl_2$, 1.1 $MgCl_2$, 11.9 $NaHCO_3$, 0.33 NaH_2PO_4, and 11.2 dextrose, pH 7.4) and pinned to a SYLGARD (Dow Corning Corporation, Midland, MI) chamber containing the Tyrode's solution and bubbled with a mixture of 95% O_2 and 5% CO_2. Intracellular potentials and currents were recorded using an Axon900A (Molecular Devices, Sunnyvale, CA) amplifier and borosilicate microelectrodes were prepared using the Flaming/Brown Micropipette Puller Model P-87 (Sutter Instruments), filled with a solution 3M KCl and were later beveled using the BV-10 Micro-Pipette Beveler (Sutter Instruments) to improve

morphology and clamp efficiency with a resistance raging from 5–15 MΩ choosing the lowest in resistance for the current electrode. Using the TEVC, miniature endplate currents (MEPCs) were recorded at a holding potential of −70mV. The output of the recording instrument was filtered at 1 kHz analog to digital converter using a Digidata 1440A (Molecular Devices, Sunnyvale, CA). Currents were digitized at 100μs per point and stored, captured and analyzed using pClamp10.3 software (Molecular Devices, Sunnyvale, CA). The miniature end plate currents were analyzed using the mini analysis program (Synaptosoft Inc., Fort Lee New Jersey). Finally, the amplitude, time constant and frequency for the recorded MEPCs were fitted and graphed to address the open channel blocker effect of fluoxetine on SCS panel. Endplates from untreated εL269F SCS transgenic mice with WT-like miniature kinetics were excluded from further analysis.

Treadmill gait analysis

Mouse gait analysis was performed via the DigiGait Imaging System (Mouse Specifics, Inc., Boston) as described previously (6). Briefly, mice walked on a motor-driven treadmill with a transparent treadmill belt. A high frame rate camera was focused on the ventral plane of the mice as they walked within an acrylic chamber, ~5 cm wide by ~25 cm long. Due to the remarkable reduction of muscle strength in mSCS, brake time was primarily selected as the most sensitive metric to demonstrate functional improvement of treated muscle in mSCS. The treadmill speed was set to 25 cm/s. Approximately 5 seconds of video were collected for each walking mouse to provide ~20 sequential strides. The right hind limb from every mSCS was measured at pre- and post-treatment with fluoxetine, in which mSCS administrated with saline was selected as control group.

Statistics

Values were represented as the mean ± STDEV. Data were analyzed using Student's *t*-test and Chi-square test where appropriate, and non-parametric Mann-Whitney *u*-test, for comparisons of percentages and ratio values, as indicated in figure legends.

Results

Fluoxetine lowers the εL269F MEPC time constant *in vitro*

We investigated the effect of fluoxetine on neuromuscular transmission in mSCS mice using TEVC by acutely exposing voltage-clamped muscle fibers to a range of physiological fluoxetine concentrations (22–24), 0.3, 0.9 and 1.5 μM by bath application. As reported previously, decay phases of MEPCs from untreated mSCS mice were nearly eight-fold longer than control mice and MEPC amplitudes were reduced by 31%. After application of fluoxetine MEPCs showed a concentration-dependent reduction in the time constant (τ_s), which averaged to 55.60 ± 17.95, 52.48 ± 22.26, 54.56 ± 22.04 and 22.80 ± 13.59 ms, in mock-treated, 0.3, 0.9 and 1.5 μM respectively (Figure 1 A, B). The decay phases could be resolved into two exponents (τ_1 and τ_2) with τ_2 showing a concentration dependent reduction, which averaged in a control SCS transgenic mice 83.82 ± 14.99 ms, whereas 78.20 ± 23.57 in 0.3 μM treatment, 75.17 ± 15.47 in 0.9 μM treatment and 56.75 ± 10.63 in 1.5 μM treatment (Figure 1 C). Fluoxetine concentrations that reduced MEPC decay time by 3.3–fold did not affect the MEPC amplitude (Figure 1D). Similarly, the MEPC frequencies

remained unaffected by the treatment since no significant difference could be detected between the untreated and fluoxetine-treated at three concentrations (Figure 1E). These results suggest that fluoxetine treatment *in vitro* significantly reduces open time of mutant nAChR channels without influencing other physiological properties.

Fluoxetine improves neuromuscular transmission and functional recovery in SCS transgenic mice

Weakness and fatigability in SCS and other NMJ disorders arise from impaired synaptic transmission associated with decremental compound muscle action potential (CMAP) amplitudes evoked by repetitive nerve stimulation (rsEMG). mSCS mice expressing different SCS mutations exhibit decremental responses to rsEMG (3,4,6,15). We investigated whether fluoxetine treatment would improve decrement in rsEMG. 9 days after fluoxetine treatment, we found a dose-dependent reduction in decrement of rsEMG in mSCS mice. Treatment of εL269F mice with 2.4 μg/g fluoxetine led to a mean decrement of 13.6±2.5%, with a dose of 4.8 μg/g the decrement was 10.3±3.2%, with 7.2 μg/g, the decrement was 4.0±1.7% and with 9.6 μg/g mean decrement was 2.8±1.0%, compared with 19.7±2.3% in untreated εL269F mice. Similar results were also seen in treated δS268F, in which reduction of decrement was 10.9±1.2% after 4.8 μg/g, 6.8±0.5% after 7.2 μg/g, and 4.2±0.6% after 9.6 μg/g treatment, compared with 18.8±3.1% in untreated δS268F mice (Figure 2; n=7; $p<0.001$).

To investigate whether fluoxetine treatment led to improved motor performance in mSCS muscle, we used a computerized, video-assisted treadmill (DigiGait@, MouseSpecifics), which allows comparison of motor behavior using individual limb of each mouse with several performance parameters, including: “brake time”, “stride length”, and “stride frequency”. Previous studies showed that “brake time” was the most sensitive parameter for detection of improved muscle function in mSCS εL269F with different treatments (6). We tested whether fluoxetine treatment of mSCS εL269F mice, the more severely affected mouse line, improved motor function, with evaluations standardized to the right hind limb. We found that fluoxetine treatment significantly reduced brake time, to nearly half of pre-treatment measurements (23±4 vs 37±3ms; $p<0.001$) to a level comparable to that of WT mice (Figure 3A; n=7). The stride length in untreated mSCS mice was 4.5 cm compared with 3.7 cm in WT mice (n=6; $p<0.001$). Fluoxetine treatment significantly reduced the mean stride length to 3.0 cm at the highest dose (Figure 3B; n=7; $p<0.001$). The mean stride frequency in mSCS mice was $5.2s^{-1}$ compared with $6.4s^{-1}$ in WT mice (n=7; $p<0.001$). Fluoxetine increased the mean stride frequency to $6.9s^{-1}$ in mSCS (Figure 3C; n=7; $p<0.001$). These findings demonstrate the functional benefit of fluoxetine treatment to the neuromuscular system by improved neuromuscular transmission in SCS, although tissue studies are needed to explore the neuroprotective effect of fluoxetine.

Fluoxetine inhibits pathological Ca^{2+} overload at endplates in mSCS

Based on the effect of fluoxetine on mutant AChR gating we hypothesized that this drug would reduce pathological accumulation of postsynaptic Ca^{2+} at the NMJ (3,6). We administered fluoxetine intraperitoneally daily to mSCS mice (εL269F and δS268F) over a range of doses (2.4, 4.8, 7.2, and 9.6 μg/g). Control mSCS mice were treated with saline or

not at all. Nine days later, we examined Ca^{2+} overload in TA muscle sections using the glyoxal bis 2-hydroxyanil (GBHA) histochemical stain (25,26). Ca^{2+} was present at mSCS endplates, but not in WT TA muscle (Figure 4; left). After 9-day treatment of εL269F, Ca^{2+}-overloaded endplates were significantly decreased in 7.2 μg/g (15.8±2.3%) and 9.6 μg/g (11.9±4.2%), compared with 38.2±2.6% in control group (Figure 4; middle; n=5; $p<0.001$). Similar results were also observed in δS268F mice, in which GBHA-labeled endplates were reduced to 17.4±0.8% and 6.1±1.7% in 7.2 μg/g and 9.6 μg/g treatments, respectively, compared with 44.3±2.7% in control group (Figure 4; right; n=7; $p<0.001$). Other doses have no effects on mSCS muscle. These results suggest that reducing open time of mutant AChRs significantly reduces Ca^{2+} overload at NMJs in mSCS muscle.

Fluoxetine prevents cysteine protease activation in mSCS

We reported previously that both calpain and caspase proteases are activated at NMJs in mSCS, to an extent comparable to the endplate Ca^{2+} overload (6–9). Therefore, we hypothesized that fluoxetine would also reduce these protease activities in mSCS muscle. We found that fluoxetine significantly reduced accumulation of active caspases in mSCS muscle. In untreated εL269F mice, 45.9% and 45.2% of endplates were labeled intensely for active caspase-3 and active caspase-9, respectively. In εL269F mice treated with increasing doses of fluoxetine, activated caspases were detected at progressively fewer endplates, from 35.2% and 37.3% for caspase-3 and caspase-9, respectively, at a dose of 2.4 μg/g to 18.2% and 16.1% caspase-3 and caspase-9, respectively at a dose of 9.6 μg/g (Figure 5A; $p<0.001$). Similar results were also found in δS268F mice, in which a dosedependent reduction in activated caspase labeling occurred to 18.3% and 16.7% of endplates labeled at the maximum dose of 9.6μg/g, compared with 48.3% and 42.8% endplates for caspase-3 and caspase-9, respectively, in the control group ($p<0.001$). The proportions of active caspase-labeled endplates are roughly equivalent to the proportion of Ca^{2+}-overloaded endplates in untreated mice.

To detect calpain and caspase-3/-9 activities in mSCS muscle, we employed a luciferase-based luminogenic caspase substrate assay (Calpain-Glo, Caspase-9-Glo and Caspase-3-Glo, Promega) to study TA muscle homogenates. In untreated εL269F mice, calpain activity was 4.2-fold of WT, whereas caspase-3 and -9 activities were 2.7- and 2.1-fold of WT, respectively. Treatment of εL269F with fluoxetine (9.6 μg/g) significantly reduced calpain activity (by 2.2-fold) and caspase-3 and -9 activities by 1.3-fold, nearly to WT levels (Figure 5B-left; n=5; $p<0.01$). Similarly, calpain activity in untreated δS268F was 5.5-fold over WT and caspase-3/-9 activities were 3.1- and 2.4-fold over WT, respectively, while after 9.6μg/g treatment calpain activity was reduced by 2.1-fold, and caspase-3 and -9 activities were reduced by 1.5-fold and 1.2-fold respectively, again similar to WT (Figure 5B-right; n=7; $p<0.01$). These results suggest that fluoxetine-mediated reduction of Ca^{2+} overload at endplates significantly diminishes activation and accumulation of cysteine proteases, calpain, caspase-3 and -9 in mSCS muscle.

Fluoxetine prevents subsynaptic DNA damage in mSCS

We previously showed that subsynaptic nuclear degeneration in patients with SCS and in mSCS was associated with DNA damage indicated by TUNEL labeling or by

phosphorylation of histone H2AX (pH2AX) at ser139, a histone modification that initiates DNA damage repair in association with activation of Ca^{2+}-activated degenerative enzymes (6,27,28). Based on the effect of fluoxetine on mutant AChRs, Ca^{2+} overload and protease activation in mSCS we investigated whether this treatment could reduce histological evidence of DNA damage (6,27). As noted previously, immunolabeling of pH2AX was present selectively at subsynaptic nuclei of mSCS muscle, labeling approximately 37% and 45% of NMJs in both εL269F and δS268F mice, respectively, similar to the numbers seen for GBHA and activated caspase labeling, (Figure 5C; $p<0.001$). However, fluoxetine significantly reduced the proportion of pH2AX-labeled NMJs to 16.1±2.8% and 37.3±2.1% with 7.2μg/g treatment in εL269F and δS268F muscle, respectively, and to 14.3±3.7% and 16.6±1.5% with 9.6μg/g treatment, respectively (Figure 5C; $n=5–7$; $p<0.001$). Collectively, these findings demonstrate that the drug fluoxetine, presumably because of its role as a non-specific ion channel blocker, prevents Ca^{2+} overload at NMJs through mutant AChRs, diminishes activation of cysteine proteases and reduces DNA damage in subsynaptic nuclei in SCS.

Discussion

Detailed studies of the slow-channel syndrome and its transgenic mouse models have revealed a complex cascade of pathological events that ensue from the genetic perturbation of ion channel function, including Ca^{2+} overload, activation of cysteine proteases and DNA and organellar damage in the subsynaptic region of the NMJ. While each of these pathological steps is a potential therapeutic target, the prospect of selective of pharmacological blockade of mutant AChRs may offer the most disease-specific strategy for intervention.

In this study, we showed that fluoxetine treatment (1.5 μM) *in vitro* considerably reduces and effectively normalizes prolonged synaptic currents (MEPC decay time) in muscle of mice expressing mutant nAChRs without affecting synaptic current strength (MEPC amplitude). This effect, seen in also cultured cells also, has been attributed to the preferential blockade by open channel blockers of ion channels with prolonged open times (11). The benefit of such a pharmacological endpoint has been translated to the successful treatment of patients with SCS using fluoxetine (11,13).

We investigated for evidence of long term, neuroprotective benefit using transgenic mice. After treating mice for 9 days mouse motor strength for mice expressing either of two SCS mutations was improved in a dose-dependent fashion as assessed using a treadmill test (Figure 3). This clinical improvement could be attributed at least in part to improvement in neuromuscular transmission as rsEMG demonstrated a dose-dependent improvement in the decremental responses in both transgenic lines (Figure 2).

While the clinical and electrophysiological findings demonstrate improvement of neuromuscular function in experimental SCS, supporting clinical experience, they do not provide evidence for long-term benefit in SCS, a degenerative disease of the NMJ. Because the principal mediator of the degenerative process appears to be elevated Ca^{2+}, entering from the extracellular space through mutant AChRs, and from internal stores through the

IP_3R_1 when activated by the binding of Ca^{2+} and IP_3 (3,6), we investigated the ability of fluoxetine to reduce subsynaptic Ca^{2+} overload. Fluoxetine had a dose-dependent reduction in the proportion of NMJs in which histological evidence of Ca^{2+} could be detected in mice expressing either SCS mutation (Figure 4). Furthermore, because Ca^{2+} is implicated in activation of downstream proteolytic enzymes in degenerative processes, and there is pronounced activation of cysteine proteases in SCS muscle (6–9,17,28), we tested whether the reduction in endplate Ca^{2+} overload following fluoxetine treatment was accompanied by changes in the elevated activity of proteases. Fluoxetine treatment markedly decreased postsynaptic caspase-3 and -9 activities, and the tissue activities of both these caspases as well as calpain in both transgenic lines in a dosedependent fashion (Figure 5). Finally, the endpoint of the degenerative process in SCS is pronounced organellar damage, leading to an appearance of a localized apoptotic process affecting mitochondria and nuclei. In SCS and its mouse model subsynaptic nuclei in the NMJ are labeled using the TUNEL assay as well as for phosphorylated H2AX, a marker of double stranded DNA damage (8,9,17,27). We found that after nine days of treatment of mSCS mice with increasing doses of fluoxetine there was a dose-dependent reduction in the proportion of subsynaptic nuclei in the NMJ demonstrating DNA damage (Figure 5).

These findings demonstrate that fluoxetine treatment provides not only for functional improvement, but dramatically reduces the biochemical and cellular measures of degeneration in the neuromuscular system in SCS, consistent with a mechanistic basis of pharmacological correction the genetic perturbation of AChR gating and prevention of the downstream consequences of cationic overload. These results suggest that SCS patients will achieve neuroprotective benefit from long-term with fluoxetine or other open ion channel blockers.

Acknowledgements

This work is supported by NIH Grant RO1 NS33202 (C.M.G.).

References

1. Engel AG, Lambert EH, Mulder DM, Torres CF, Sahashi K, Bertorini TE, Whitaker JN. A newly recognized congenital myasthenic syndrome attributed to a prolonged open time of the acetylcholine-induced ion channel. Annals of neurology. 1982; 11:553–569. [PubMed: 6287911]
2. Gomez CM, Maselli R, Gammack J, Lasalde J, Tamamizu S, Cornblath DR, Lehar M, McNamee M, Kuncl RW. A betasubunit mutation in the acetylcholine receptor channel gate causes severe slow-channel syndrome. Annals of neurology. 1996; 39:712–723. [PubMed: 8651643]
3. Gomez CM, Maselli RA, Groshong J, Zayas R, Wollmann RL, Cens T, Charnet P. Active calcium accumulation underlies severe weakness in a panel of mice with slow-channel syndrome. The Journal of neuroscience. 2002; 22:6447–6457. [PubMed: 12151524]
4. Gomez CM, Maselli RA, Vohra BP, Navedo M, Stiles JR, Charnet P, Schott K, Rojas L, Keesey J, Verity A, et al. Novel delta subunit mutation in slow-channel syndrome causes severe weakness by novel mechanisms. Annals of neurology. 2002; 51:102–112. [PubMed: 11782989]
5. Zayas R, Groshong JS, Gomez CM. Inositol-1,4,5- triphosphate receptors mediate activity-induced synaptic Ca2+ signals in muscle fibers and Ca2+ overload in slow-channel syndrome. Cell calcium. 2007; 41:343–352. [PubMed: 16973214]

6. Zhu H, Bhattacharyya BJ, Lin H, Gomez CM. Skeletal muscle IP3R1 receptors amplify physiological and pathological synaptic calcium signals. The Journal of neuroscience. 2011; 31:15269–15283. [PubMed: 22031873]
7. Groshong JS, Spencer MJ, Bhattacharyya BJ, Kudryashova E, Vohra BP, Zayas R, Wollmann RL, Miller RJ, Gomez CM. Calpain activation impairs neuromuscular transmission in a mouse model of the slowchannel myasthenic syndrome. The Journal of clinical investigation. 2007; 117:2903–2912. [PubMed: 17853947]
8. Zhu H, Bhattacharyya BJ, Lin H, Gomez CM. Skeletal muscle calpain acts through nitric oxide and neural miRNAs to regulate acetylcholine release in motor nerve terminals. The Journal of neuroscience. 2013; 33:7308–7324. [PubMed: 23616539]
9. Zhu H, Pytel P, Gomez CM. Selective inhibition of caspases in skeletal muscle reverses the apoptotic synaptic degeneration in slow-channel myasthenic syndrome. Human molecular genetics. 2014; 23:69–77. [PubMed: 23943790]
10. Fukudome T, Ohno K, Brengman JM, Engel AG. AChR channel blockade by quinidine sulfate reduces channel open duration in the slow-channel congenital myasthenic syndrome. Annals of the New York Academy of Sciences. 1998; 841:199–202. [PubMed: 9668240]
11. Harper CM, Fukodome T, Engel AG. Treatment of slowchannel congenital myasthenic syndrome with fluoxetine. Neurology. 2003; 60:1710–1713. [PubMed: 12771277]
12. Chaouch A, Muller JS, Guergueltcheva V, Dusl M, Schara U, Rakocevic-Stojanovic V, Lindberg C, Scola RH, Werneck LC, Colomer J, et al. A retrospective clinical study of the treatment of slow-channel congenital myasthenic syndrome. Journal of neurology. 2012; 259:474–481. [PubMed: 21822932]
13. Colomer J, Muller JS, Vernet A, Nascimento A, Pons M, Gonzalez V, Abicht A, Lochmuller H. Long-term improvement of slow-channel congenital myasthenic syndrome with fluoxetine. Neuromuscular disorders : NMD. 2006; 16:329–333. [PubMed: 16621558]
14. Finlayson S, Spillane J, Kullmann DM, Howard R, Webster R, Palace J, Beeson D. Slow channel congenital myasthenic syndrome responsive to a combination of fluoxetine and salbutamol. Muscle & nerve. 2013; 47:279–282. [PubMed: 23281026]
15. Gomez CM, Maselli R, Gundeck JE, Chao M, Day JW, Tamamizu S, Lasalde JA, McNamee M, Wollmann RL. Slow-channel transgenic mice: a model of postsynaptic organellar degeneration at the neuromuscular junction. The Journal of neuroscience. 1997; 17:4170–4179. [PubMed: 9151734]
16. Gomez CM, Maselli R, Williams JM, Bhattacharyya BB, Wollmann RL, Day JW. Genetic manipulation of AChR responses suggests multiple causes of weakness in slow-channel syndrome. Annals of the New York Academy of Sciences. 1998; 841:167–180. [PubMed: 9668235]
17. Vohra BP, Groshong JS, Zayas R, Wollmann RL, Gomez CM. Activation of apoptotic pathways at muscle fiber synapses is circumscribed and reversible in a slow-channel syndrome model. Neurobiology of disease. 2006; 23:462–470. [PubMed: 16815027]
18. Mulder KJ, Mulder JB. Ketamine and xylazine anesthesia in the mouse. Veterinary medicine, small animal clinician : VM**SAC. 1979; 74:569–570.
19. Kashiwa HK, House CM Jr. The Glyoxal Bis(2-Hydroxyanil) Method Modified for Localizing Insoluble Calcium Salts. Stain technology. 1964; 39:359–367. [PubMed: 14226919]
20. Koelle GB, Friedenwald JA. A histochemical method for localizing cholinesterase activity. Proceedings of the Society for Experimental Biology and Medicine. Society for Experimental Biology and Medicine. 1949; 70:617–622.
21. Lee SG, Su ZZ, Emdad L, Sarkar D, Franke TF, Fisher PB. Astrocyte elevated gene-1 activates cell survival pathways through PI3K-Akt signaling. Oncogene. 2008; 27:1114–1121. [PubMed: 17704808]
22. Amsterdam JD, Fawcett J, Quitkin FM, Reimherr FW, Rosenbaum JF, Michelson D, Hornig-Rohan M, Beasley CM. Fluoxetine and norfluoxetine plasma concentrations in major depression: a multicenter study. The American journal of psychiatry. 1997; 154:963–969. [PubMed: 9210747]
23. Goodnick PJ. Pharmacokinetics of second generation antidepressants: fluoxetine. Psychopharmacology bulletin. 1991; 27:503–512. [PubMed: 1813897]

24. Grajales-Reyes GE, Baez-Pagan CA, Zhu H, Grajales-Reyes JG, Delgado-Velez M, Garcia-Beltran WF, Luciano CA, Quesada O, Ramirez R, Gomez CM, et al. Transgenic mouse model reveals an unsuspected role of the acetylcholine receptor in statin-induced neuromuscular adverse drug reactions. The pharmacogenomics journal. 2013; 13:362–368. [PubMed: 22688219]

25. Kawabuchi M. Neostigmine myopathy is a calcium ion-mediated myopathy initially affecting the motor end-plate. Journal of neuropathology and experimental neurology. 1982; 41:298–314. [PubMed: 6804607]

26. Leonard JP, Salpeter MM. Agonist-induced myopathy at the neuromuscular junction is mediated by calcium. The Journal of cell biology. 1979; 82:811–819. [PubMed: 511934]

27. Rogakou EP, Nieves-Neira W, Boon C, Pommier Y, Bonner WM. Initiation of DNA fragmentation during apoptosis induces phosphorylation of H2AX histone at serine 139. The Journal of biological chemistry. 2000; 275:9390–9395. [PubMed: 10734083]

28. Vohra BP, Groshong JS, Maselli RA, Verity MA, Wollmann RL, Gomez CM. Focal caspase activation underlies the endplate myopathy in slow-channel syndrome. Annals of neurology. 2004; 55:347–352. [PubMed: 14991812]

Highlights

1. First demonstration at the synaptic level of neuroprotection of a genetic degenerative disease.
2. Confirms more than functional improvement, i.e., neuroprotection in a human disease model.
3. Two distinct genetic lines gave virtually identical results.
4. Model serves as a preclinical pipeline for short and long term testing of potential treatments.

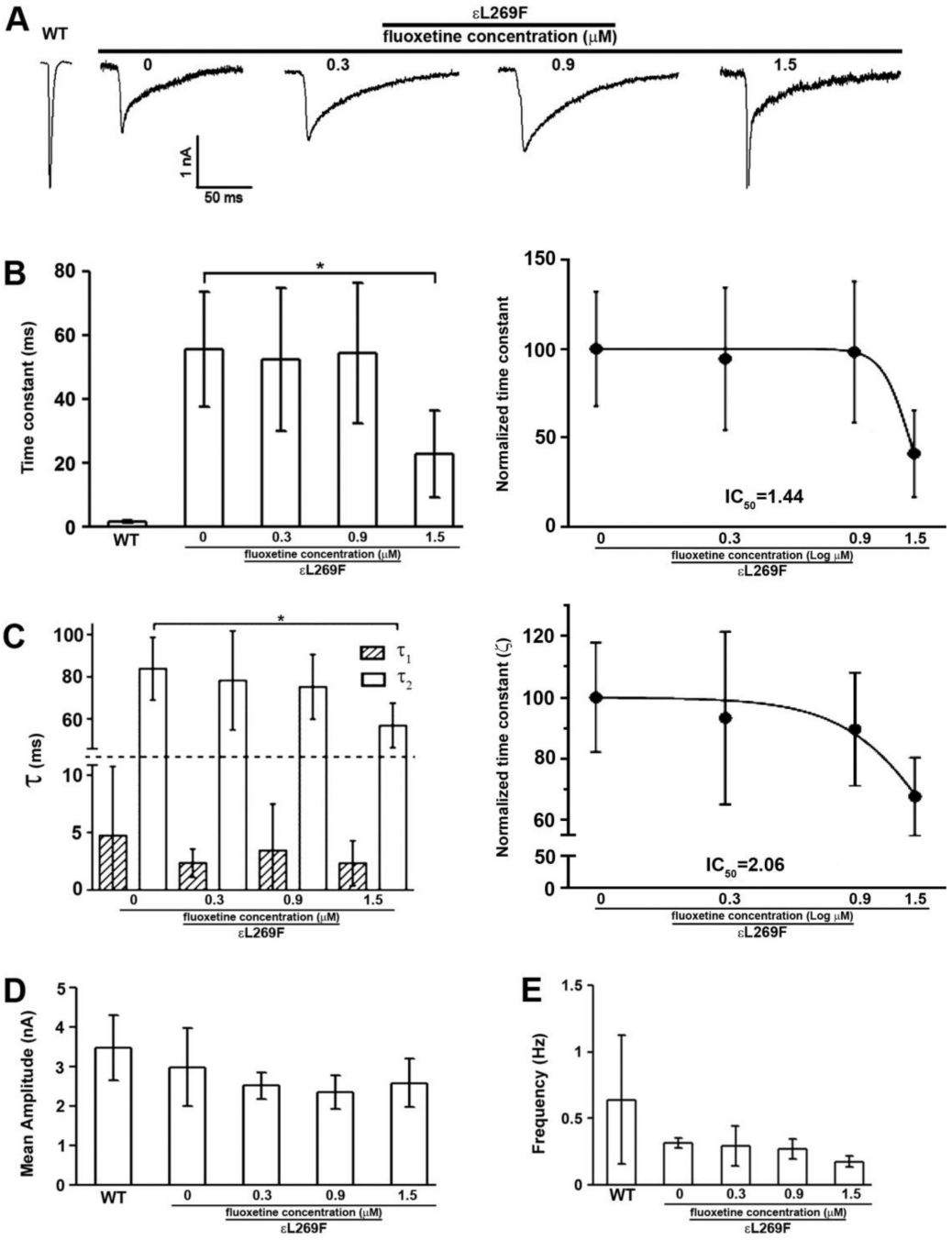

Figure 1. Fluoxetine treatment corrects altered mSCS εL269F nAChR kinetics

Two-electrode voltage clamp (TEVC) recordings of quantal activity for from wild type and εL269F mice diaphragms treated acutely with fluoxetine at concentrations of 0.3, 0.9 and 1.5 μM. **A**. The decay time constant in control SCS transgenic mice was 55.60 ± 17.95 ms whereas 52.48 ± 22.26 in 0.3 μM treatment, 54.56 ± 22.04 in 0.9 μM treatment and 22.80 ± 13.59 in 1.5 μM treatment. **B**. The MEPC time constant was dramatically reduced in SCS transgenic mice with 1.5 μM treatment. **C**. Decay phases were resolved into two exponents (τ_1 and τ_2) with τ_2 showing a concentration dependent reduction. n=4, **p*<0.05. Student's *t*-

test. **D** and **E**. Neither mean amplitude nor the frequency of MEPCs recorded from εL269F mice was affected by fluoxetine. n=4; Student's *t*-test.

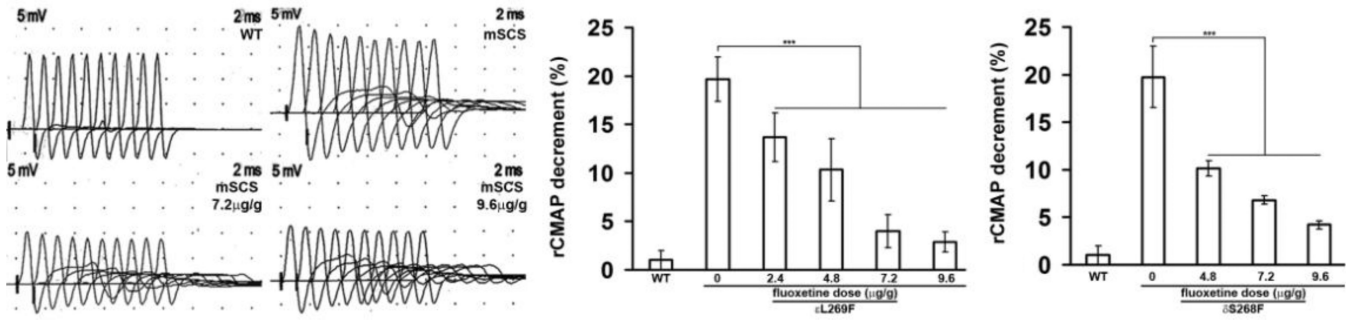

Figure 2. Decremental responses in rsEMG in mSCS with fluoxetine treatment

Left. Compound muscle action potentials (CMAP) recorded during repetitive stimulation (rsEMGs) in WT, untreated mSCS and mSCS treated with fluoxetine. Decremental responses were seen in mSCS while reduced decremental responses were shown in mSCS (εL269F) with fluoxetine treatment of 7.2 and 9.6μg/g. **Middle.** εL269F mice with 2.4 μg/g fluoxetine reduced decrement to 13.6±2.5% whereas decrement was 10.3±3.2% with 4.8 μg/g fluoxetine, 4.0±1.7% with 7.2 μg/g fluoxetine, and 2.8±1.0% with 9.6 μg/g treatment, compared with 19.7±2.3% in untreated εL269F mice. **Right.** To treated δS268F, decrement was 10.9±1.2% after 4.8 μg/g fluoxetine, 6.8±0.5% after 7.2 μg/g, and 4.2±0.6% after 9.6 μg/g treatment, compared with 18.8±3.1% in untreated δS268F mice. n=7; ***p<0.001, all comparisons were analyzed by Student's *t*-test.

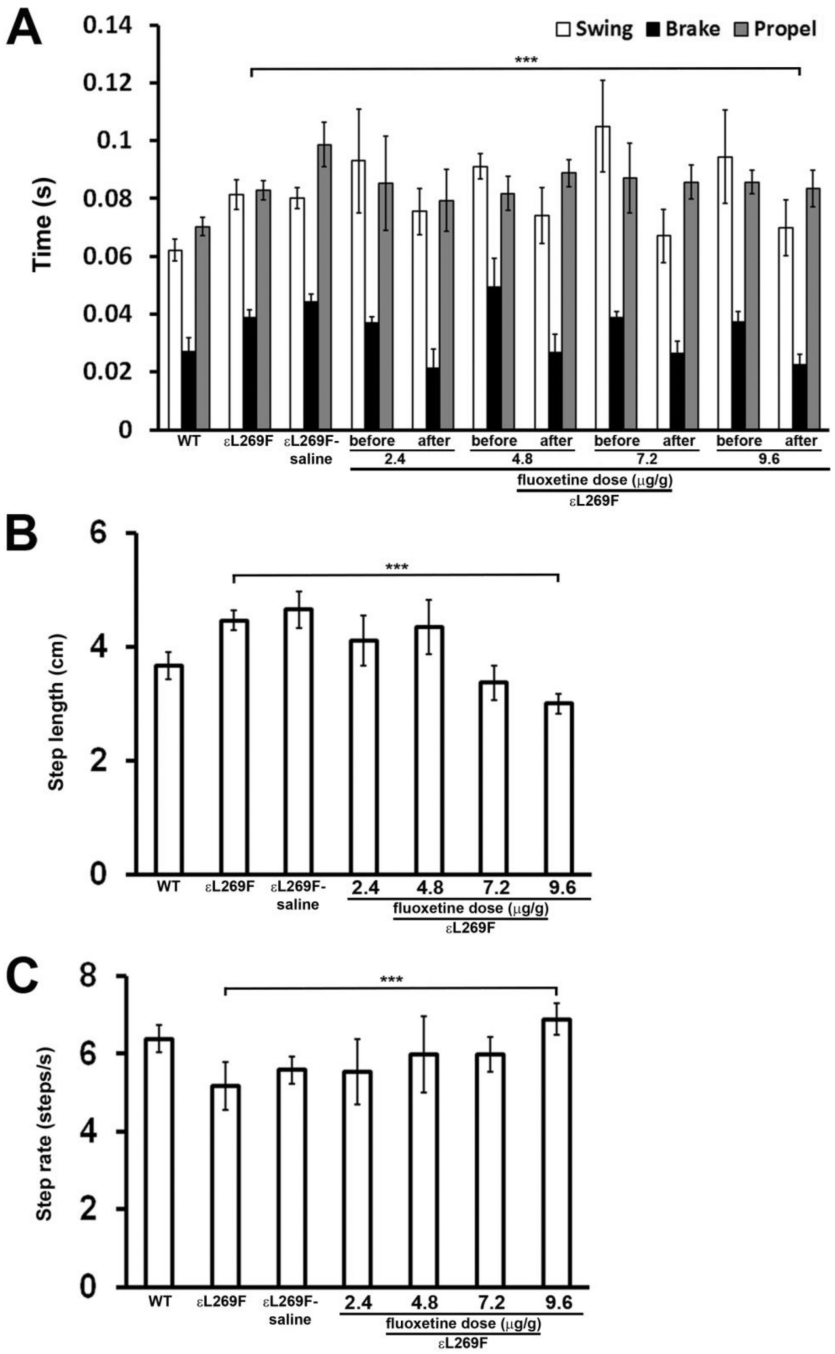

Figure 3. Fluoxetine treatment improves motor function in mSCS (εL269F)

A. Right hindlimb motor time interval parameters measured in motorized treadmill (DIGIgait®) in WT and mSCS and mSCS treated fluoxetine. Functional parameters termed “swing”, “brake” and “propel” are time intervals for three components of normal leg movements recorded doing walking, as defined in methods are identical between left and right hindlimb in WT mice. All three parameters are symmetrically and significantly increased at right hindlimbs in pre-treated mSCS mice and control mSCS treated with saline (mSCS-saline) comparison to WT. After fluoxetine treatment, brake time from the identical

pre-treated hindlimbs is significantly reduced in treated mSCS whereas no statistical difference is found in the time of propel and swing. n=7; ***p<0.001, Student's t-test.

B. Mean hindlimb stride length in WT and mSCS and mSCS treated with fluoxetine. The average stride length for both limbs in mSCS (4.46±0.18) and mSCS control (4.65±0.31) is significantly longer than WT (3.67±0.24). Fluoxetine treatment reduces mean stride length to 3.0±0.17 in treated mSCS. n=7; ***p<0.001, Student's *t*-test.

C. Mean step frequency in WT and mSCS and mSCS treated with fluoxetine. The average step frequency for both limbs in mSCS (5.18±0.62) and mSCS control (5.58±0.35) is significantly lower than WT (6.38±0.34). Fluoxetine treatment increases mean step frequency to 6.88±0.4 in treated mSCS. n=7; ***p<0.001, Student's *t*-test.

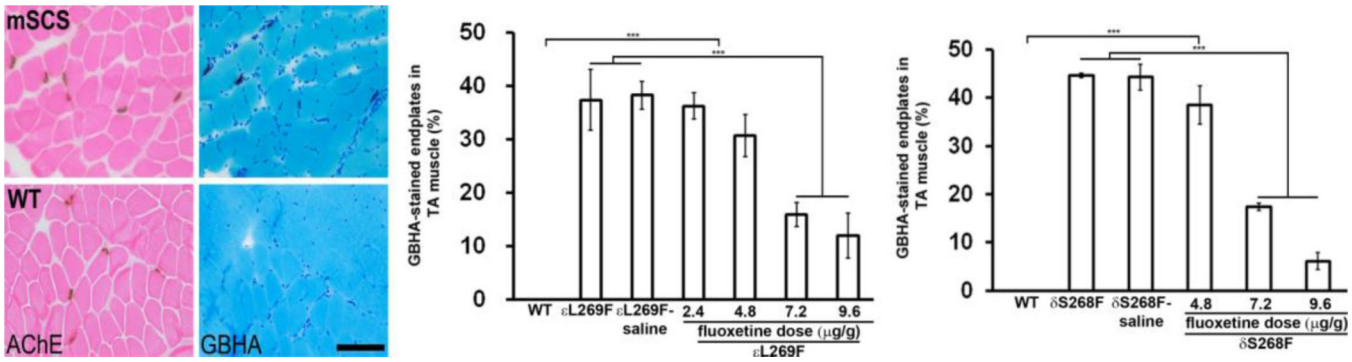

Figure 4. Fluoxetine prevents Ca^{2+} overload of NMJs in mSCS

Left. Serial TA muscle sections labeled for cholinesterase (dark brown) to localize endplates and GBHA (red) to localize Ca^{2+} overloading in WT and mSCS. Ca^{2+} overloading was found at endplates of mSCS, but not in wild type (WT). Scale bar=60μm. **Middle.** Quantitation of Ca^{2+}-overload of endplates (% GBHA-labeled endplates) in WT and in untreated mSCS mice (εL269F) and) with treatment of serial concentrations of fluoxetine. Endplates from WT TA showed no Ca^{2+}-labeled endplates, while a significant number of NMJ were overloaded with Ca^{2+} in untreated εL269F (37.3±5.7%) and control εL269F treated with saline (mSCS (εL269F)-saline; 38.2±2.6%) whereas Ca^{2+}-overloaded endplates were significantly decreased in 7.2 μg/g (15.8±2.3%) and 9.6 μg/g (11.9±4.2%) treatment. **Right.** The similar results were also shown in mSCS mice (δS268F). Compared with δS268F (44.7±0.5%) and control δS268F (44.3±2.7%), treated δS268F with a dose of 7.2 and 9.6 μg/g reduced Ca^{2+}-labeled endplates to 17.4±0.8% and 6.1±1.7%, respectively. n=5–7; ***p<0.001. All comparisons were analyzed by Student's *t*-test.

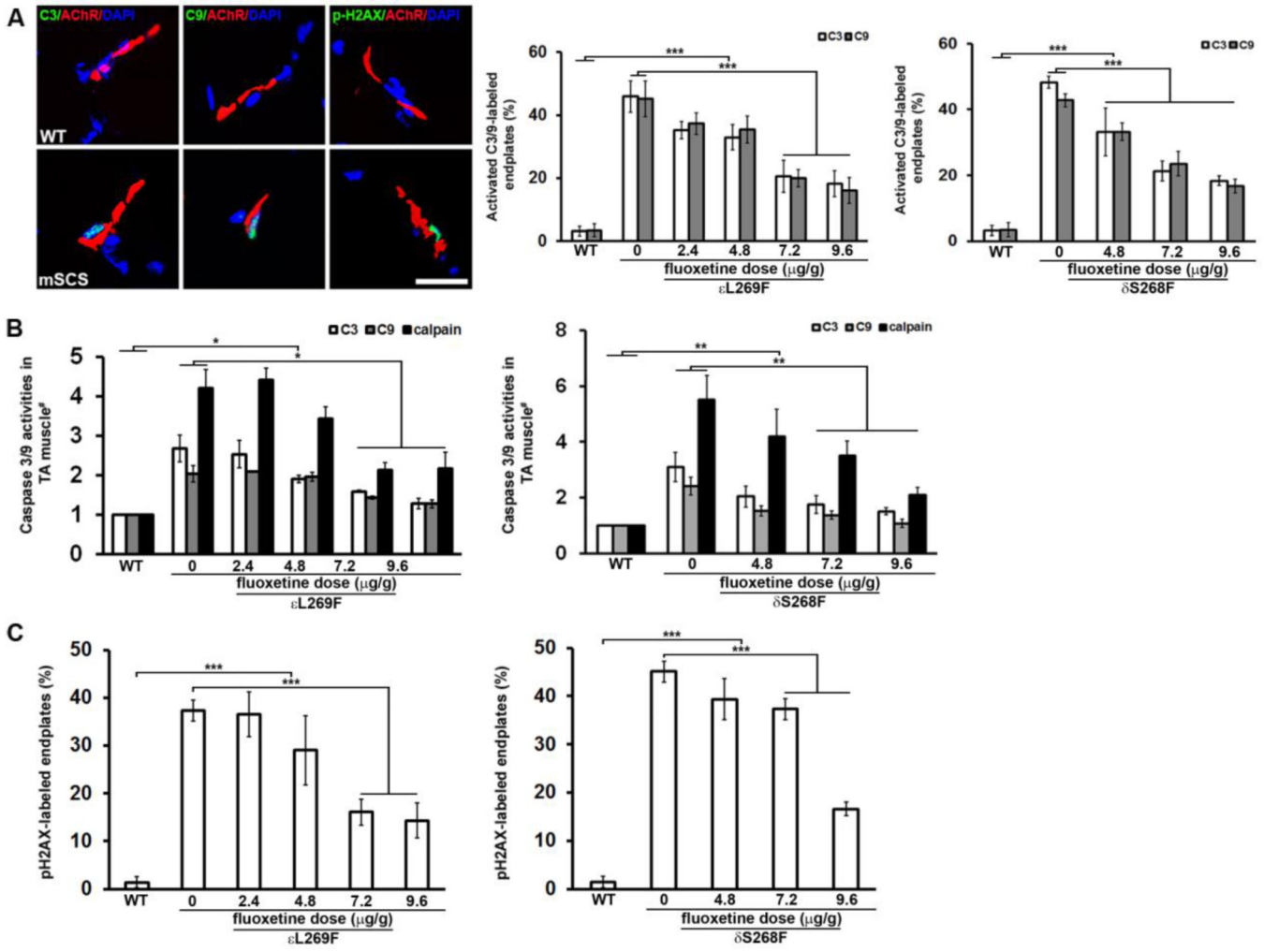

Figure 5. Fluoxetine prevents pathological activation of calpain, caspase-3 and caspase-9 at NMJs, and subsynaptic DNA damage in mSCS

A. Left. Co-localization of activated caspase-3 (green, arrows) and caspase-9 (green, arrows) with NMJs (red) in WT and mSCS. Activated caspase-3 and caspase-9 are seen in mSCS NMJ with subsynaptic nuclei, but are not seen in WT. Ca^{2+}-mediated DNA damage in subsynaptic nuclei was exhibited as co-localization of phospho-H2AX-labeled (pH2AX, green) nuclei (DAPI, blue) with NMJ (red) in untreated mSCS. n=5; Scale bar=15μm. **Middle.** Quantitation of endplates labeled with activated caspase-3 and caspase-9 in WT, untreated mSCS (εL269F) and mSCS (εL269F) treated with fluoxetine under indicated conditions. In untreated mSCS (εL269F) 45.9±5.0% of endplates were labeled with cleaved caspase-3 and 45.2±5.9% with cleaved caspase-9, while no active caspases were detected in WT endplates. Treatment of mSCS (εL269F) muscle with 9.6μg/g fluoxetine significantly reduced labeling for cleaved caspase-3 (18.2±4.1%) and caspase-9 (16.1±4.1%). **Right.** Compared with cleaved caspase-3 (48.3±1.8%) and cleaved caspase-9 (42.8±2.0%) in untreated mSCS (δS268F), fluoxetine treatment with 9.6μg/g significantly reduced labeling for cleaved caspase-3 and caspase-9 to 18.3±1.5% and 16.7±2.1%, respectively. n=5; ***p<0.001. All comparisons were analyzed by Student's *t*-test.

B. Relative activity of calpain, caspase-3 and caspase-9 proteases (# = normalized to WT) for untreated mSCS and treated mSCS muscle under indicated conditions. **Left.** Protease activities for untreated mSCS (εL269F) muscle are 4.2-fold (calpain), 2.7-fold (caspase-3), and 2.0-fold (caspase-9) to WT activity while reduced protease activities of 2.2-fold (calpain), 1.3-fold (caspase-3) and 1.3-fold (caspase-9) in εL269F treated with 9.6μg/g fluoxetine. n=5; *p<0.05. **Right.** Protease activities for untreated mSCS (δS268F) muscle are 5.5-fold (calpain), 3.1-fold (caspase-3), and 2.4-fold (caspase-9) to WT activity while reduced protease activities of 2.1-fold (calpain), 1.5-fold (caspase-3) and 1.2-fold (caspase-9) in mSCS (δS268F) with 9.6μg/g fluoxetine treatment. n=7; **p<0.01. All comparisons were analyzed by Mann-Whitney *u*-test.

C. Quantitation of pH2AX-labeled NMJs in WT, untreated mSCS and mSCS treated with fluoxetine under indicated conditions. **Left.** In WT NMJ pH2AX-labeled nuclei were rare (1.4±1.2%). In untreated mSCS (εL269F) a significant number of NMJ nuclei were labeled with pH2AX (37.3±2.2%). Treatment of mSCS (εL269F) with 9.6μg/g fluoxetine significantly reduced pH2AX-labeling to 14.3±3.7%. **Right.** In untreated mSCS (δS268F) a significant number of NMJ nuclei were labeled with pH2AX (45.1±2.3%). Treatment of δS268F with 9.6μg/g fluoxetine significantly reduced pH2AX-labeling to 16.6±1.5%. εL269F=5; δS268F=7; ***p<0.001. All comparisons were analyzed by Student's *t*-test.